PCCP

Cite this: *Phys. Chem. Chem. Phys.*, 2011, **13**, 18179–18185

www.rsc.org/pccp

PAPER

Spontaneous oscillations of cell voltage, power density, and anode exit CO concentration in a PEM fuel cell

Hui Lu,*[ab] Liisa Rihko-Struckmann*[a] and Kai Sundmacher[ac]

Received 17th June 2011, Accepted 26th August 2011
DOI: 10.1039/c1cp21984g

The spontaneous oscillations of the cell voltage and output power density of a PEMFC (with PtRu/C anode) using CO-containing H_2 streams as anodic fuels have been observed during galvanostatic operating. It is ascribed to the dynamic coupling of the CO adsorption (poisoning) and the electrochemical CO oxidation (reactivating) processes in the anode chamber of the single PEMFC. Accompanying the cell voltage and power density oscillations, the discrete CO concentration oscillations at the anode outlet of the PEMFC were also detected, which directly confirms the electrochemical CO oxidation taking place in the anode chamber during galvanostatic operating.

1. Introduction

Low temperature PEM fuel cells (PEMFCs) have been paid much attention with regard to transportation and stationary applications.[1–12] The main challenge in the utilization of H_2-based PEMFCs is the manufacture, storage, and transport of extremely pure hydrogen (>99.999%) as an ideal fuel for PEMFCs. Thus the alternative H_2-rich reformates, produced by the off-board steam reforming, partial oxidation or auto-thermal reforming of light hydrocarbons and alcohols[7–11] would be attractive and promising fuels for PEMFCs. However, the reformate streams contain significant levels of CO aside from the main H_2 and CO_2 components. The high CO concentration can poison seriously the anode catalyst and degrade the cell performance. The CO in the reformate can be removed mostly by a high-and low-temperature CO water-gas-shift (WGS), followed by preferential oxidation (PrOx) of CO. In addition, CO in lower amounts (<10 ppm) may be tolerant by the anode catalysts, and then several basic strategies had been suggested for this case: (i) high temperature operating, (ii) air or O_2 bleeding, (iii) potential/current pulsing, and (iv) advanced alloy catalysts.[4–9] However, they generally encounter some problems, *e.g.*, long-term stability, safety issues, setup complexity, and system efficiency. Thus it is of importance to get insight into CO poisoning and its resulted dynamic properties (*e.g.*, poisoning, reactivating and oscillations) in PEMFCs so as to provide a practical guide to industrial and automotive applications.

Oscillatory phenomena were observed usually in the electrochemical oxidation of methanol, formaldehyde and formic acid on the platinum electrode, and some experimental/simulation work has been performed in these systems.[12–15] The formation and electrochemical oxidation of the strongly adsorbed and/or reactive intermediates play a crucial role for the potential oscillations. The potential oscillations, instabilities and steady-state multiplies have also been observed and simulated in PEMFCs, which are resulted generally from dynamic CO poisoning/reactivating, mass transfer limitation, and/or reactant concentration gradients.[16–27] However, there is still limited work done so far on the potential oscillations in the PEMFCs with CO-containing H_2 feed for understanding the complicated processes.

In this work, the cell voltage and output power density oscillation behavior of a fuel cell using CO-containing H_2 fuels has been investigated. The output power densities of a single fuel cell under the potential oscillatory-state are compared to those under the potential steady-state. The CO concentration oscillations at the anode outlet, accompanying the cell voltage oscillations, are also reported.

2. Experimental

MEAs (Nafion 117 membrane with an active area of 26 cm^2, 30% PtRu/C as anode catalyst with 0.75 mg cm^{-2} loading; unsupported Pt Black as cathode catalyst with 5 mg cm^{-2} loading) were prepared in-house.[22,25] The commercial catalysts were purchased from Johnson-Matthey. The graphite bipolar plates have parallel flow fields with channels of 2 mm width and 2 mm depth, with 1 mm wide ribs between them. The PEMFCs were assemblied by the gold-plated copper

[a] *Max Planck Institute for Dynamics of Complex Technical Systems, Sandtorstrasse 1, D-39106 Magdeburg, Germany. E-mail: huilu@dicp.ac.cn, rihko@mpi-magdeburg.mpg.de; Fax: +86 411 8469 4447, +49 391 6110 566; Tel: +86 411 8437 9180, +49 391 6110 318*
[b] *State Key Laboratory of Catalysis, Dalian Institute of Chemical Physics, Chinese Academy of Sciences, Dalian 116023, China*
[c] *Otto-von-Guericke University Magdeburg, Process Systems Engineering, Universitätsplatz 2, D-39106 Magdeburg, Germany*

plates as current collectors and steel stainless plates for bracing the whole sandwich structure. The experimental setup consisted of the calibrated rotameters to feed the reactant gases to the anode (the pure H_2 streams containing ppm levels of CO, f = 100–400 mL min^{-1}) and cathode (the pure O_2 stream, f = 300 mL min^{-1}) sides of the PEMFC. The H_2 streams containing various CO concentrations (50–1000 ppm) were used as anodic feeding streams. The humidification of the anode and cathode gases was conducted by bubbling the streams into water bottles. All experiments were carried out at room temperature and under atmospheric pressure.

An electrochemical workstation (IM6e, Zahner-elektrik GmbH, Germany) equipped with an external Zahner EL101 booster was used galvanostatically or potentiostatically. A multi-channel potential recorder (with a response time of 1 s) was used to record the cell voltage changes with time. An online IR CO gas analyzer (ABB Automation Products GmbH, Germany) with a measurement range of 0–250 ppm CO was used for CO concentration analysis in the anode inlet/outlet gases, and its sampling rate is 1 s. A cooling trap and a silica-gel column were used for removing vapor before permitting the streams to enter the chamber of the moisture-sensitive IR CO analyzer.

3. Results and dissussion

3.1. Cell voltage oscillations

The cell voltage was kept stable at 1.03 V during the open-circuit conditions (without current) with pure H_2 stream and H_2 streams containing 50, 100, 200 and 1000 ppm CO. However, autonomous oscillations of the cell voltage were observed when a current density of 25 mA cm^{-2} or higher was applied. Fig. 1 shows the autonomous voltage oscillation patterns (time duration: 250 s) of the fuel cell using 50, 100, 200 and 1000 ppm CO/H_2 stream as anode

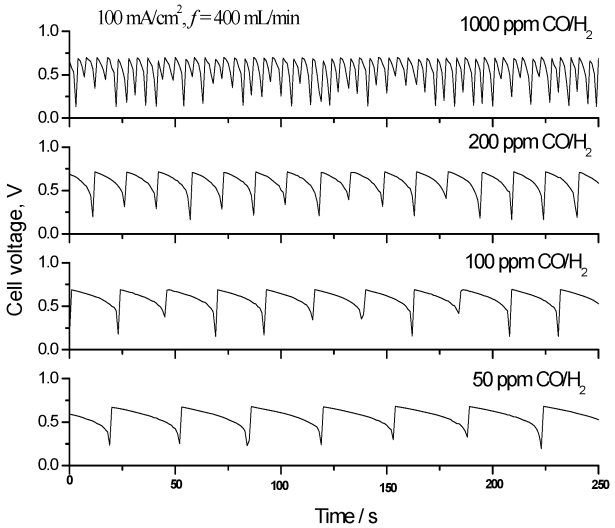

Fig. 1 Cell voltage oscillations at various CO concentrations (50–1000 ppm CO) in the anodic feeding streams at j = 100 mA cm^{-2}, f = 400 mL min^{-1}.

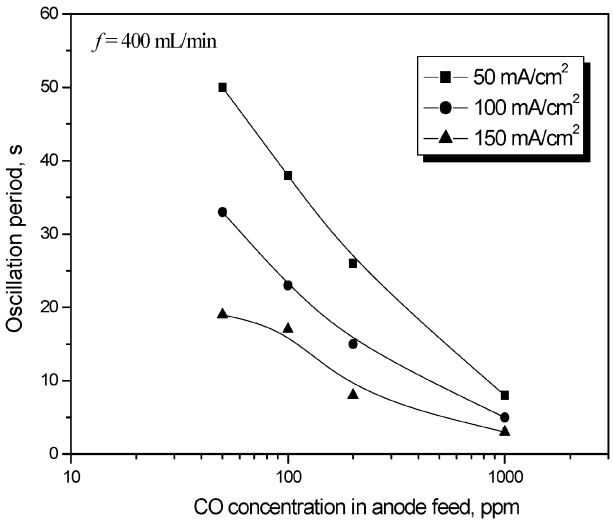

Fig. 2 Oscillation periods of the cell voltage at various CO concentrations (50–1000 ppm CO) and current densities (50–150 mA cm^{-2}).

feed at a given current density of 100 mA cm^{-2} applied. The potential oscillation periods (at given current densities) decrease with the increase of the CO concentration in the anode H_2 feed (Fig. 2). Obviously, it is the reason that faster poisoning of the anode catalyst takes place using H_2 stream containing higher levels of CO concentration, consequently resulting in the decrease of the poisoning duration in a potential oscillation cycle.

In addition, the anodic flow rate can also influence the voltage oscillations of the fuel cell. Fig. 3 shows the effects of the anodic flow rates on the cell voltage oscillations (time duration: 250 s) at a given current density of 100 mA cm^{-2} using 200 ppm CO/H_2 stream. The oscillation periods of the cell voltage decrease expectedly with the increase of the anodic flow rate from 100 to 400 mL min^{-1} (see Fig. 4). It is due to a faster poisoning process with a higher flow rate in a potential oscillation cycle, similarly as discussed with the H_2 streams containing various CO concentrations. Moreover, at high flow rates (300 and 400 mL min^{-1}), similar oscillation periods were observed. Fig. 5 gives the oscillations of the cell voltage (time duration: 250 s) at different current densities for 100 ppm and 200 ppm CO/H_2 streams. The oscillation periods of the cell voltage decrease monotonously with the increase of the current density applied in the fuel cell.

The oscillation patterns of the cell voltage describe clearly the dynamic coupling of the CO adsorption and the electro-oxidation processes on the surface of the PtRu/C anode catalyst. Initially, the fuel cell can generate the desired current at a high cell voltage (*i.e.* low anodic over-potential) at low CO coverage. With the increasing of the CO coverage, the cell voltage decreases due to the continuous increasing of the anode over-potential. The adsorbed CO is then oxidized from the anode catalyst surface when a certain critical potential of the electrochemical CO oxidation is attained. This dynamic process can be recycled and self-sustained.[19,22,25] Meanwhile, the oscillatory voltage also indicates the self-sustained efforts of the fuel cell to recover the poisoned active sites of the anode catalyst for maintaining given current densities.

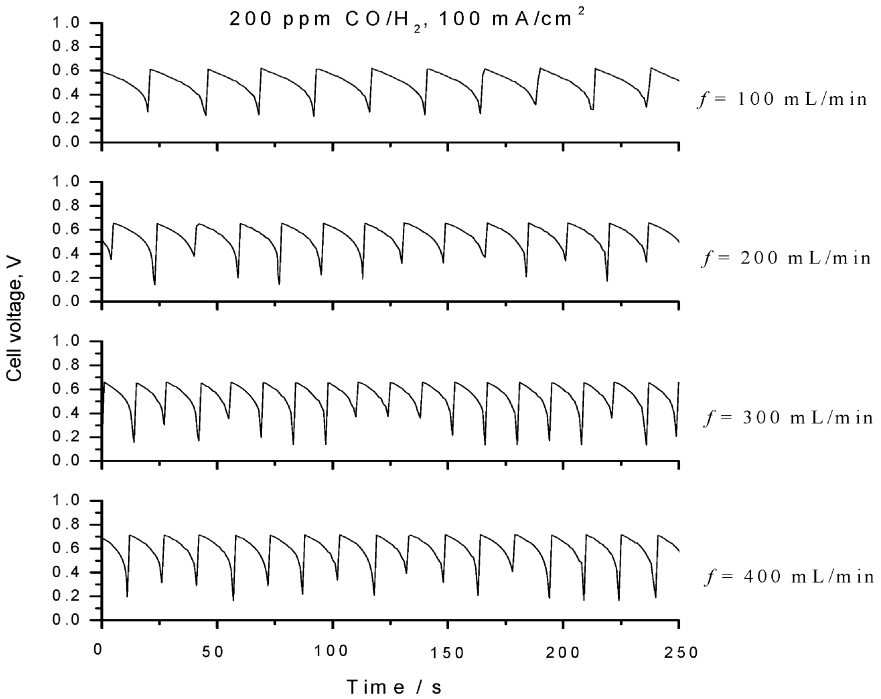

Fig. 3 Cell voltage oscillations at various flow rates (100–400 mL min^{-1}) using 200 ppm CO/H_2 as an anodic feeding stream, j = 100 mA cm^{-2}.

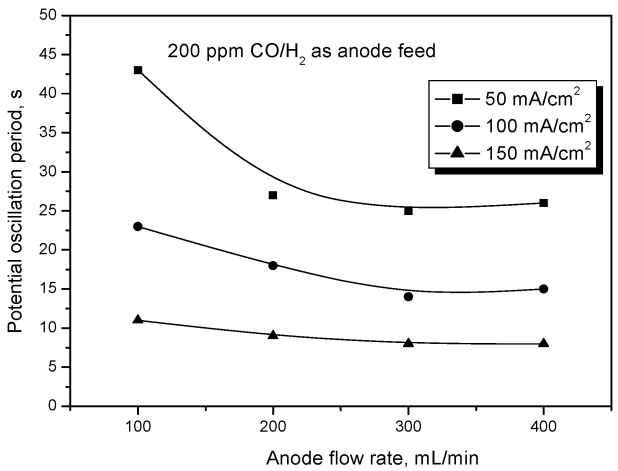

Fig. 4 Oscillation periods of the cell voltage at various flow rates (100–400 mL min^{-1}) and current densities (50–150 mA cm^{-2}) using 200 ppm CO/H_2 as an anodic feeding stream.

3.2. Output power density oscillations

Fig. 6a shows the oscillations of the cell output power density at a current density of 50 mA cm^{-2} using 100 ppm CO/H_2 stream feeding fuel. The output power density oscillations resort to the same mechanism, which results from the electrochemical CO oxidation in the fuel cell. Power density oscillations have the same frequency as that of cell voltage oscillations in the cell system. The time-averaged output power density under potential oscillatory-state was calculated for each current density (25–200 mA cm^{-2}) for 100 ppm CO/H_2 feeding stream. Fig. 6b gives the comparison of the output power density under potentiostatic and galvanostatic modes. The time-averaged power density at each current density under galvanostatic mode is much higher than that under the potentiostatic mode. Using 200 ppm CO/H_2 stream as the feeding fuel, similar phenomena of the cell voltage oscillations and power density improvements were also observed, as seen in Fig. 7.

The improvement in the reaction rate and efficiency was gained over the steady-state system by an attempt made to accelerate the reaction rate or decrease the oxidation potential for the electrochemical oxidation of formic acid, with superimposing current/potential oscillatory signals.[28,29] The biochemical system efficiency can also be enhanced within the autonomous oscillations themselves.[30] The enhanced output power density in the oscillatory cell is consistent with the oscillations appearing due to the self-sustained efforts by the whole system to maximize efficiency.[22,25,31,32] Obviously, the improved output power densities result from the decreased anode averaged over-potential. The CO poisoning process is relatively very slow on a seconds (s) timescale, but the electrochemical CO oxidation process is relatively very quick on a milliseconds (ms) timescale. Although they are regular for the potential cycles, the cell voltage changes are not symmetric, and then resulting in the asymmetric output power density, as shown in Fig. 6a and 7a.

3.3. Anode exit CO concentration oscillations

The anode outlet CO concentrations were measured online at various current densities (0–200 mA cm^{-2}). When lower current densities (<100 mA cm^{-2}) were applied for 100 ppm CO/H_2 feeding stream, the CO concentration oscillations of the anode outlet in the fuel cell were observed notably. Fig. 8a shows the CO concentration oscillations of the anode outlet at

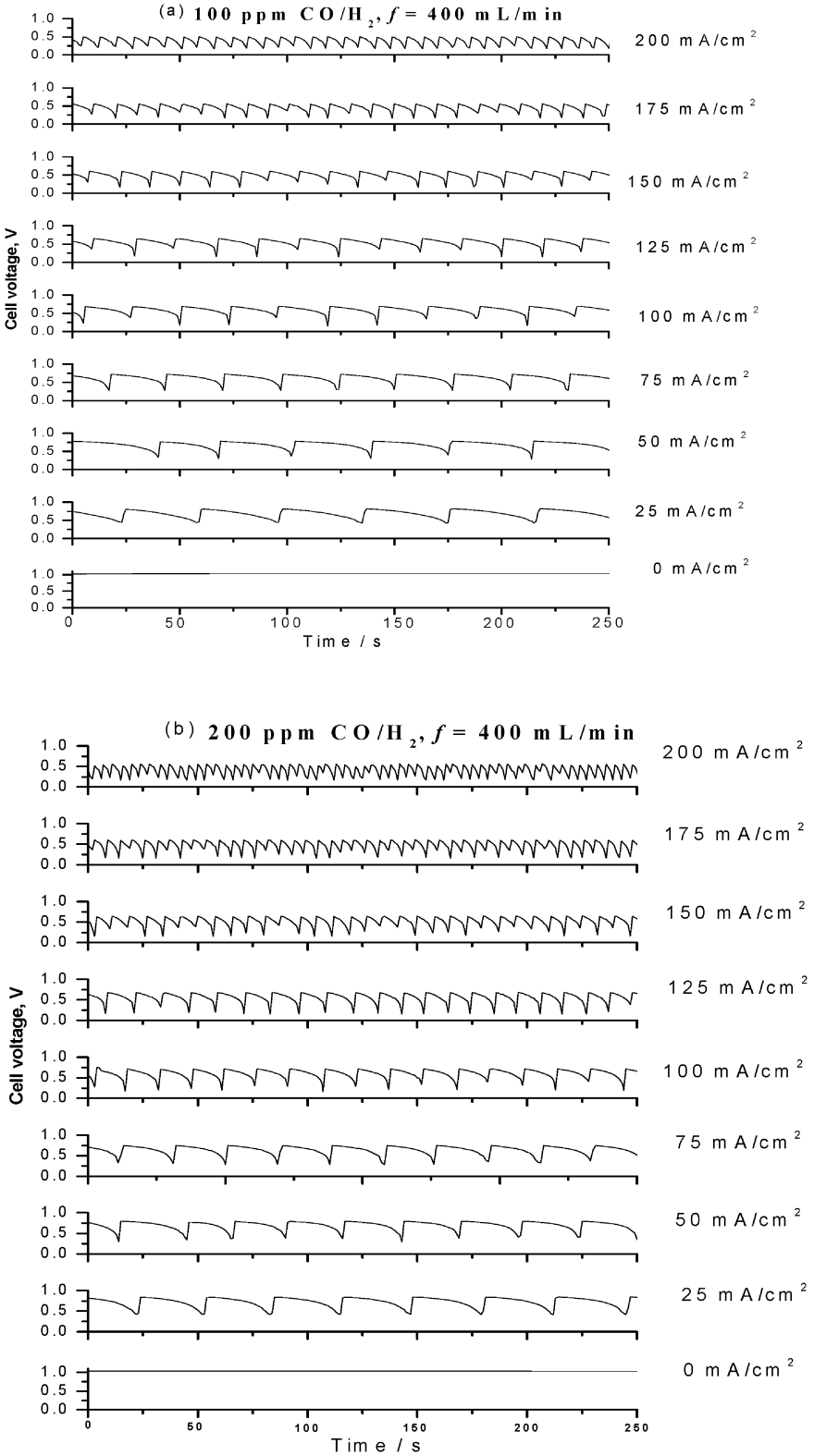

Fig. 5 Cell voltage oscillations at various current densities (0–200 mA cm^{-2}) using 100 ppm CO/H_2 (a) and 200 ppm CO/H_2 (b) as feeding streams, f = 400 mL min^{-1}.

a current density of 50 mA cm^{-2}. It demonstrates clearly the CO electrochemical oxidation in the anode flow-field chamber of the fuel cell. The anode outlet CO concentration oscillates discretely, which is different from the smooth potential oscillations (Fig. 8b). It is the reason that the anode outlet effluents were forced to go through a cooling trap and a silica-gel column for removing the water vapor completely, and then finally entering the measuring chamber of the CO analyzer.

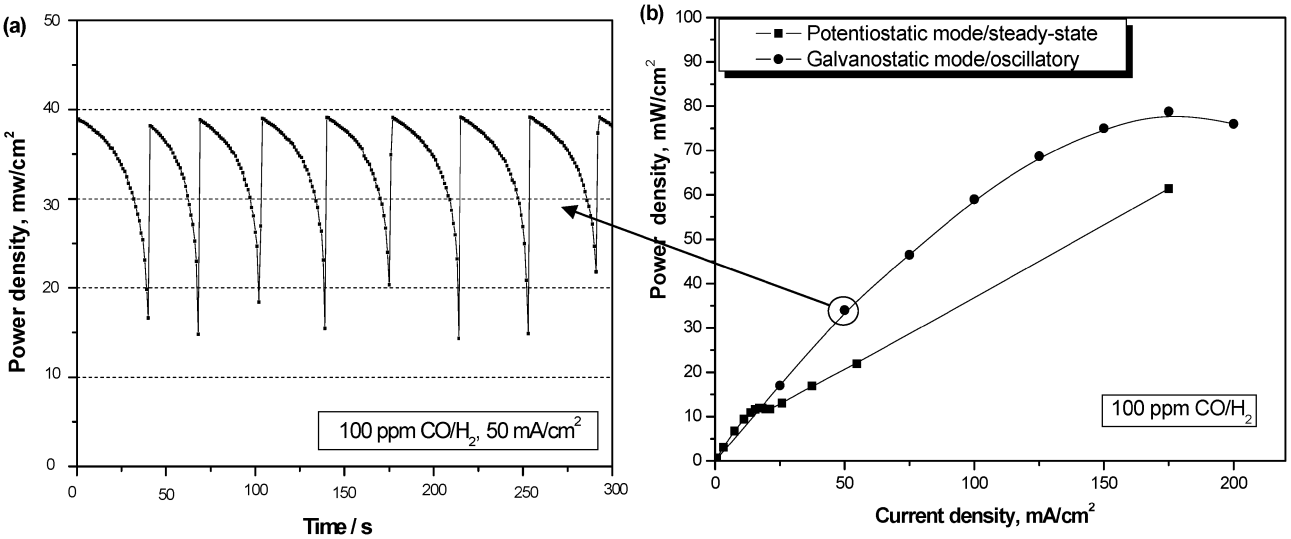

Fig. 6 Output power density oscillation (a) at $j = 50$ mA cm^{-2} and improved output power density (b) at $j = 25$–200 mA cm^{-2} of the PEMFC using 100 ppm CO/H_2 as an anodic feeding stream, $f = 400$ mL min^{-1}.

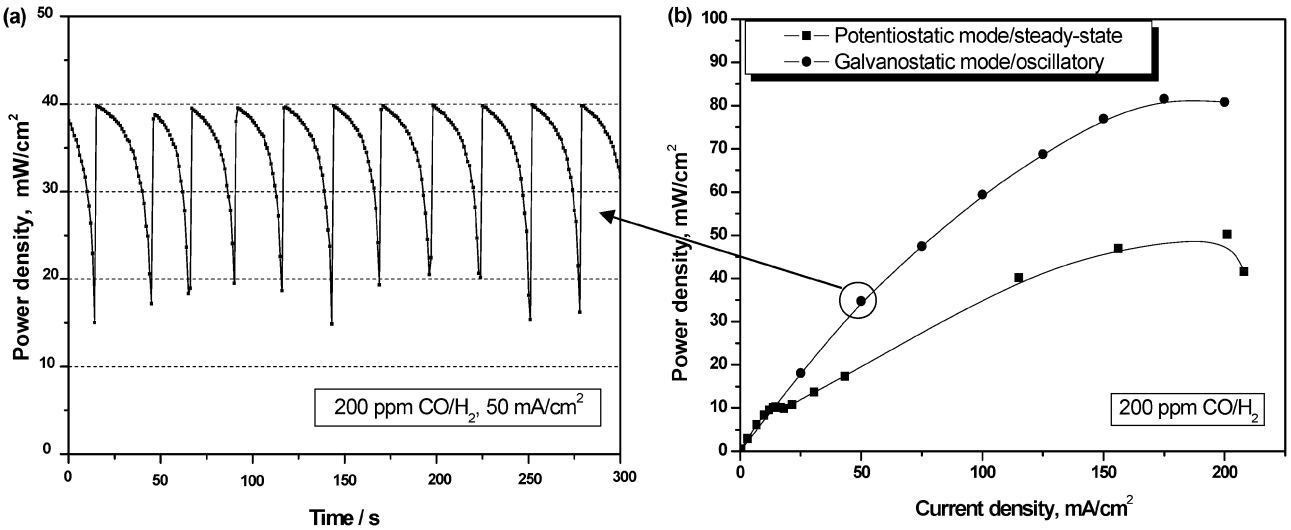

Fig. 7 Output power density oscillation (a) at $j = 50$ mA cm^{-2} and improved output power density (b) at $j = 25$–200 mA cm^{-2} of the PEMFC using 200 ppm CO/H_2 as an anodic feeding stream, $f = 400$ mL min^{-1}.

These back mixing processes could disturb seriously the continuous and oscillatory distribution of the outlet CO concentrations. Consequently, the discrete characters of CO concentration oscillations at the anode outlet were observed by the CO analyzer. Moreover, the CO concentration oscillation period of the anode outlet, is nearly close to that of the corresponding cell voltage oscillations.

For 200 ppm CO/H_2 stream as an anodic feeding fuel, similar oscillations of the anode outlet CO concentration (at 50 mA cm^{-2}) are shown in Fig. 9. The results confirm that they possess similar oscillation periods between the cell voltage oscillations and the outlet CO concentration oscillations. In addition, the oscillations of the anode outlet CO concentration of PEMFC could be observed readily at lower current densities (<100 mA cm^{-2}). The oscillation periods of the cell voltage at low current densities are longer than those at high current densities, which could reduce the scattering of concentration gradients from the anode outlet of the fuel cell to the measuring chamber of the CO analyzer.

4. Conclusions

The spontaneous oscillations of the cell voltage, the output power density, and the anode outlet CO concentration oscillations in a PEMFC were observed under the galvanostatic mode using CO-containing H_2 streams as anodic fuels. These interestingly autonomous oscillations are ascribed to the dynamic coupling of the CO poisoning and the electrochemical CO reactivating processes taking place in the anode chamber of the fuel cell. The averaged output power density during galvanostatic operating is much higher than that during potentiostatic operating at given current densities (25–200 mA cm^{-2}). The anode outlet

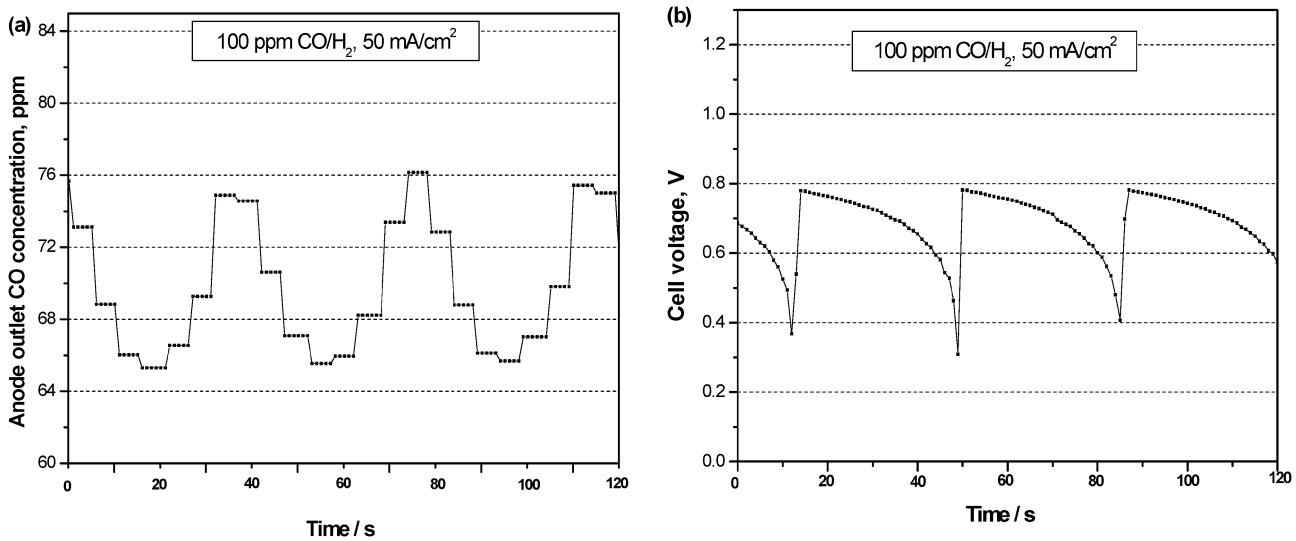

Fig. 8 Anode outlet CO concentration oscillations (a) and the corresponding cell voltage oscillations (b) using 100 ppm CO/H_2 as an anodic feeding stream, $j = 50$ mA cm^{-2}, $f = 400$ mL min^{-1}.

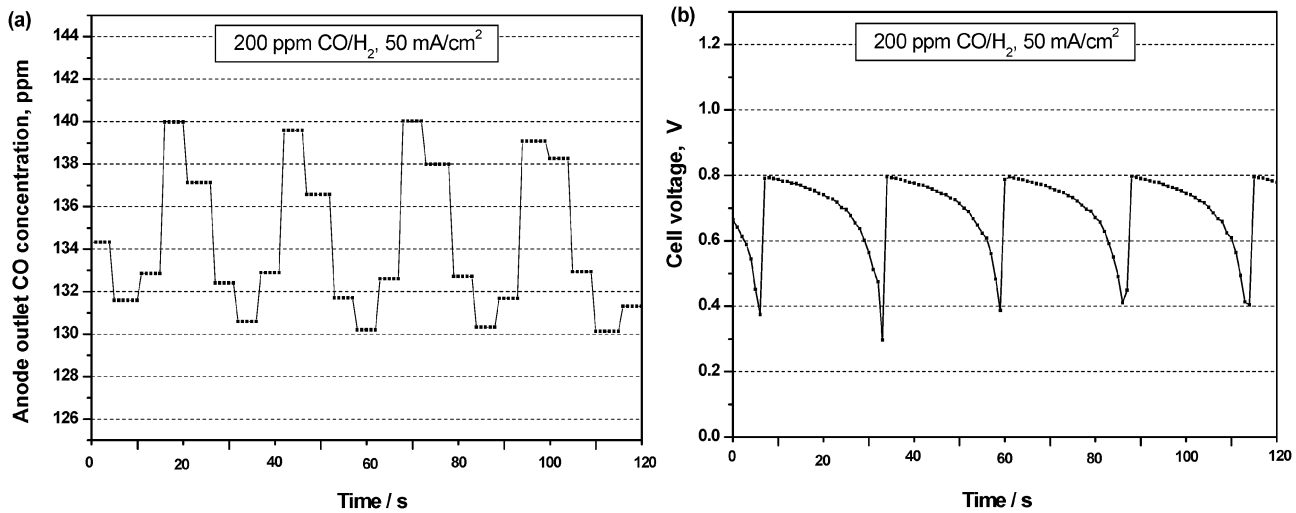

Fig. 9 Anode outlet CO concentration oscillations (a) and the corresponding cell voltage oscilations (b) using 200 ppm CO/H_2 as an anodic feeding stream, $j = 50$ mA cm^{-2}, $f = 400$ mL min^{-1}.

CO concentration oscillations demonstrate directly that the electrochemical oxidation of CO took place in the anode flow-field of the PEMFC during galvanostatic operating.

Acknowledgements

H.L. is grateful for support from a Max Planck Scholarship funded by the Max-Planck-Gesellschaft. The financial support for this work obtained from the co-operation project (*ProBio*) between the Fraunhofer Gesellschaft and the Max Planck Gesellschaft is gratefully acknowledged.

References

1 J. H. Wee and K. Y. Lee, *J. Power Sources*, 2006, **157**, 128.
2 C. Z. He, H. R. Kunz and J. M. Fenton, *J. Electrochem. Soc.*, 2001, **148**, A1116.
3 B. Lakshmanan, W. Huang and J. W. Weidner, *Electrochem. Solid-State Lett.*, 2002, **5**, A267.
4 T. Ioroi, T. Akita, S. I. Yamazaki, A. Siroma, N. Fujiwara and K. Yasuda, *Electrochim. Acta*, 2006, **52**, 491.
5 S. Litster and K. G. McLean, *J. Power Sources*, 2004, **130**, 61.
6 U. Eberle and R. von Helmolt, *Energy Environ. Sci.*, 2010, **3**, 689.
7 C. P. Huang, R. C. Jiang, M. Elbaccouch, N. Muradov and J. Fenton, *J. Power Sources*, 2006, **162**, 563.
8 S. Jimenez, J. Soler, R. X. Valenzuela and L. Daza, *J. Power Sources*, 2004, **151**, 69.
9 K. Scott, S. Pilditch and M. Mamlouk, *J. Appl. Electrochem.*, 2007, **37**, 1245.
10 M. De Falco, *Fuel*, 2011, **90**, 739.
11 L. C. Carrette, K. A. Friedrich, M. Huber and U. Stimming, *Phys. Chem. Chem. Phys.*, 2001, **3**, 320.
12 J. Lee, C. Eickes, M. Eiswirth and G. Ertl, *Electrochim. Acta*, 2002, **47**, 2297.
13 M. Kikuch, W. Kon, S. Miyahara, Y. Mukouyama and H. Okamoto, *Electrochim. Acta*, 2007, **53**, 846.
14 M. Kikuchi, S. Miyahara, Y. Mukouyama and H. Okamoto, *J. Phys. Chem.*, 2008, **112**, 7186.
15 A. Miki, S. Ye and M. Osawa, *J. Electroanal. Chem.*, 2004, **563**, 23.
16 M. Murthy, M. Esayian, A. Hobson, S. MacKenzie, W. K. Lee and J. W. Van Zee, *J. Electrochem. Soc.*, 2001, **148**, A1141.

17 Z. G. Qi, C. Z. He and A. Kaufman, *J. Power Sources*, 2002, **111**, 239.
18 A. A. Kulikovsky, H. Scharmann and K. Wippermann, *Electrochem. Commun.*, 2004, **6**, 729.
19 J. X. Zhang and R. Datta, *J. Electrochem. Soc.*, 2004, **151**, A689.
20 A. Katsaounis, S. Balomenou, D. Tsiplakides, M. Tsampas and C. G. Vayenas, *Electrochim. Acta*, 2005, **50**, 5132.
21 A. Katsaounis, S. Balomenou, D. Tsiplakides, S. Brosda, S. Neophytides and C. G. Vayenas, *Appl. Catal., B*, 2005, **56**, 251.
22 H. Lu, L. Rihko-Struckmann, R. Hanke-Raschenbach and K. Sundmacher, *Electrochim. Acta*, 2009, **54**, 1184.
23 A. H. Thomason, T. R. Lalk and A. J. Appleby, *J. Power Sources*, 2004, **135**, 204.
24 C. G. Farrell, C. L. Gardner and M. Ternan, *J. Power Sources*, 2007, **171**, 282.
25 H. Lu, L. Rihko-Struckmann, R. Hanke-Raschenbach and K. Sundmacher, *Top. Catal.*, 2008, **51**, 89.
26 P. P. Lopes, E. A. Ticianelli and H. Varela, *J. Power Sources*, 2011, **196**, 84.
27 S. Kirsch, R. Hanke-Raschenbach and K. Sundmacher, *J. Electrochem. Soc.*, 2011, **158**, B44.
28 R. R. Adzic, K. I. Popov and M. A. Pamic, *Electrochim. Acta*, 1978, **23**, 1191.
29 M. Schell, F. N. Albahadily and J. Safar, *J. Electroanal. Chem.*, 1993, **353**, 303.
30 J. G. Lazar and J. Ross, *J. Chem. Phys.*, 1990, **92**, 3579.
31 J. X. Zhang and R. Datta, *Electrochem. Solid-State Lett.*, 2004, **7**, A37.
32 J. X. Zhang and R. Datta, *J. Electrochem. Soc.*, 2005, **152**, A1180.